Synthesis and characterization of some C-Ti based multilayer and composite nanostructures

V. Ciupina[a,e], C. P. Lungu[b], R. Vladoiu[a], G. C. Prodan[a], C. Porosnicu[b], E. Vasile[c], M. Prodan[a], V. Nicolescu[d], V. Dinca[a], O. Cupsa[d], A. Velea[f], R. Manu[g,*]
[a]*Ovidius University of Constanta, 124 Mamaia Avenue, Constanta, Constanta, Romania 900527*
[b]*National Institute for Lasers, Plasma and Radiation Physics, P.O. Box MG-36, 077125 Bucharest Romania*
[c]*University Politehnica of Bucharest, Faculty of Applied Chemistry and Material Science,Department of Oxide Materials and Nanomaterials, No. 1–7 Gh. Polizu Street, Bucharest 011061, Romania*
[d]*CERONAV Constanta, Pescarilor Street no. 69A, 900581 Constanta, Romania*
[e]*Academy of Romanian Scientists, Splaiul Independentei No. 54, Bucharest 050094, Romania*
[f]*National Institute for Materials Physics, Atomistilor No. 405, 077125, Magurele, Romania*
[g]*National Institute for Marine Research and Development "Grigore Antipa" 300 Mamaia Avenue, Constanta, Romania 90058*

Carbon-Titanium multilayer and composite thin films were obtained by Thermionic Vacuum Arc (TVA) method. The nanostructured films consisted by a carbon base layer and seven alternatively Titanium and Carbon layers were deposed on Silicon substrate. As well, to give C-Ti multilayer films with different percentages in Ti and C of layers, a thick Carbon base layer was deposed on Si substrate, and then seven Ti-C layers. In order to achieve the successively layers with C, and Ti different percentages, were adjusted the discharge parameters of C and Ti plasma sources to obtain the desired composition of layers. By changing of substrate temperature, and on the other hand the bias potential up to –700V, different batches of samples were obtained. Characterization of structural properties of films was achieved by Grazing Incidence X-ray Diffraction (GIXRD) and Electron Microscopy technique (TEM). The measurements show that increase of the substrate temperature reveal the changes in Ti_xC_y lattice parameters. The tribological measurements were performed using a ball-on-disk system with normal forces of 0.5, 1, 2, 3N respectively and a Bruker Hystrion TI 980 TriboIndenter. Was found that the coefficient of friction depends on the synthesis temperature, bias voltage and also by the C content, Ti content and amount of TiC nanocrystallites. To characterize the electrical conductive properties, the electrical surface resistance versus temperature have been measured, and then the electrical conductivity is calculated. Using the Wiedeman-Frantz law was obtained the thermal conductivity.

(Received December 2, 2021; Accepted March 17, 2022)

Keywords: TVA, C-Ti films, TEM, Tribological properties, Electrical properties

1. Introduction

Carbon-Titanium multilayer films show a growing interest lately, especially for mechanical, electrical and optical properties cosed by Titanium Carbide(TiC) phase and Ti [1-9] . Such structures can have various applications due to the possibility of changing the friction coefficient as well as due to the feasibility of switching from the semiconductor character to the metallic character and implicitly changing the sign of the coefficient of variation of the electrical resistance with temperature. The purpose of the work is to obtain and characterize C-Ti

* Corresponding author: rmanu@alpha.rmri.ro
https://doi.org/10.15251/JOR.2022.182.177

multilayers with certain properties determined by content of Ti_xC_y and Ti, using Thermionic Vacuum Arc(TVA) method [10-13]. The aim was to highlight the Ti_xC_y phases by Grazing Incidence X-ray Diffraction(GIXRD) measurements, Electron Microscopy(TEM) techniques as well as by coefficient of friction, nanoindentation and electrical conductivity measurements

2. Experimental Set-Up

To obtain high quality C-Ti multilayer thin films on Silicon substrates was used TVA method [10-13]. The experimental set-up (FIGURE 1) consist by two independent anode-cathode systems placed inside the deposition chamber. Anode was represented by the coating material and the cathode by an electron thermoemissive redhot tungsten wire. The Ti layers were obtained by placing the bulk material into thermos-resistant TiB_2 crucible and heating it until a constant vapor pressure is achieved; by increasing the high voltage applied on the material, a plasma is generated in its vapors.

In a first way of working, the coated films (samples M_1, M_2, etc.), consiste of a base layer of about 100nm thick carbon deposited on the 0.5mm thick silicon (100) substrate having the size of $12x15mm^2$. Subsequently, seven carbon and titanium layers were deposited alternatively on top of carbon base layer, each of them has a final thickness up to 40nm.

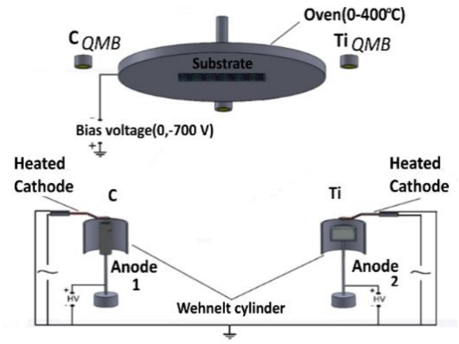

Fig 1. The experimental set-up.

In a second way of working the films (samples N_1, N_2, etc.) consiste of a 20nm carbon base layer and seven carbon-titanium layers, with different percentages in C and Ti respectively, each having a thickness of 40nm. The thickness and the distribution of C and Ti in a layer were highlighted in Table 1.

In a third deposition way the films were obtained by codeposition, the composite films having a variable C: Ti atomic ratio 9:1 at interface to 1:9 at the surface (samples C_1,C_2,etc.).

Table 1. C/Ti layer distribution.

Titanium	Thickness(nm)	Carbon	Thickness(nm)
-	-	100%	20.00
1%	1.00	99%	39.00
3%	2.30	97%	37.70
5%	4.00	95%	36.00
7%	5.00	93%	35.00
10%	7.00	90%	33.00
15%	10.00	85%	30.00
25%	16.00	75%	24.00

In a fourth deposition way, the C-Ti multilayers were constructed from the silicon substrate as follows: 100nm of carbon, followed by alternant 17nm Ti and 40 nm C three times, covered by one last 17 nm Ti layer, resulting a seven multilayer structure . For the composite layer, after the pre 100nm carbon one, we varied quasi continuously the Ti:C atomic ratio, from 1:9 and reaching 9:1 at the top of the 119 nm. For both multilayer and composite structures, in all deposition ways, several batches were obtained for comparison by changing the substrate temperature during the deposition (i.e., Room temperature,100, 200, 300 and 400°C – samples DM_1, DM_2,…, and DC_1, DC_2,…,respectively; also one deposition batch was obtained at 300°C with a -700V polarisation voltage on the substrates, in order to increase the ions energy reaching the layer, during the coating process – sample DC_6).

3. Results and Discussions

Grazing Incidence X-ray Diffraction (GIXRD).

The structural investigation of the C-Ti thin films is performed by Grazing Incidence X-ray diffraction (GIXRD) using a Rigaku SmartLab diffractometer.

In the case of multilayers sample M_6(400°C substrat deposition temperature), the crystalline phases are show in FIGURE 2. Face-centered cubic phases can be found. If the deposition parameters will be improved, and oxygen will be removed, only Ti-C face-centered cubic phases will be obtained, meaning that all titanium atoms will react with carbon atoms. It has a thickness of 71nm, according to the X-ray reflectometry (XRR) measurements.

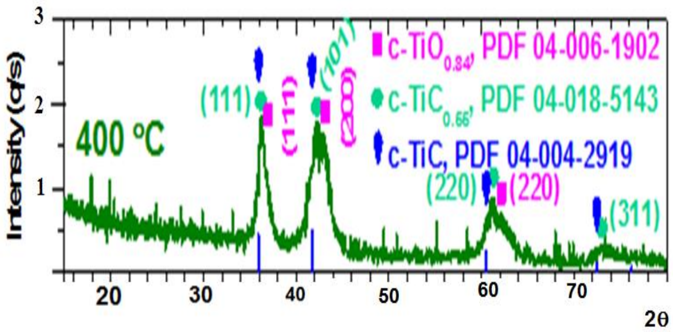

Fig. 2 . X-ray diffraction pattern for sample M_6(400°C).

For codeposition samples the crystalline phases for sample C_6(400°C) are show in FIGURE 3. A single polycrystalline phase is found (TiC0.4O0.6, face-centered cubic lattice, space group Fm-3m (225), PDF 04-021-7421).

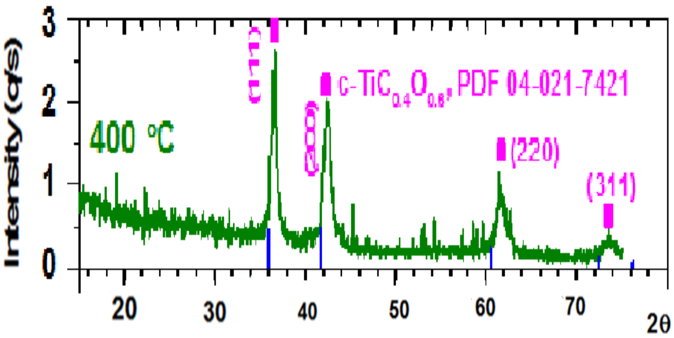

Fig. 3. X-ray diffraction patterns for codeposition sample C_6(400°C). h = Hexagonal;c = Cubic.

In the case of sample DC_4(composite layer, substrate temperature 300^0C), X-ray diffraction pattern reveal a single policrystalline phase (Ti_2C, cubic lattice, space group Fd-3m (227)) (FIGURE 4).

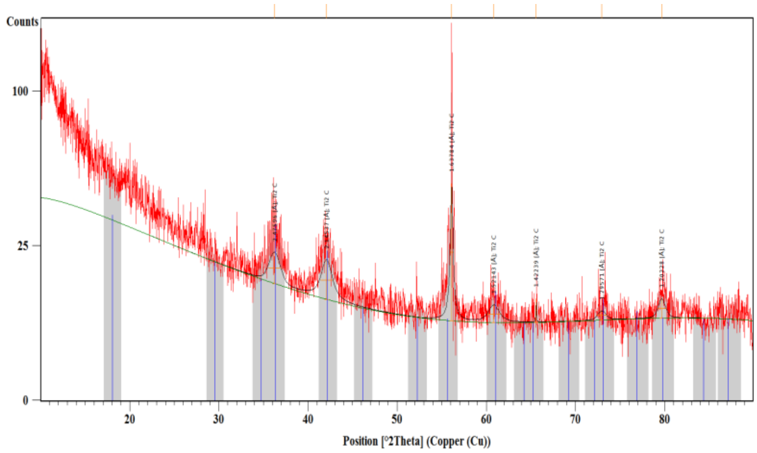

Fig. 4. X-ray diffraction pattern for composite sample DC_4.

3.1. TEM measurements

The characterization of microstructure properties of as prepared C-Ti multilayer structures were done using Electron Microscopy techniques (TEM). The microstructure properties were studies using transmission electron microscope CM120 and Philips Tecnai F30G^2 at 300kV set-up.

Analysis of diffraction patterns was performed using CRISP2 application, with the crystalline material module (ELD). The indexing of lines extracted from the profile was done by comparative method.

In FIGURE 5 is presented extracted profile from diffraction pattern for sample M_8(400°C deposition temperature). Based on appropriate polycrystalline structure of sample, are obtained the sizes of crystallites using Scherrer method (TABLE 2).

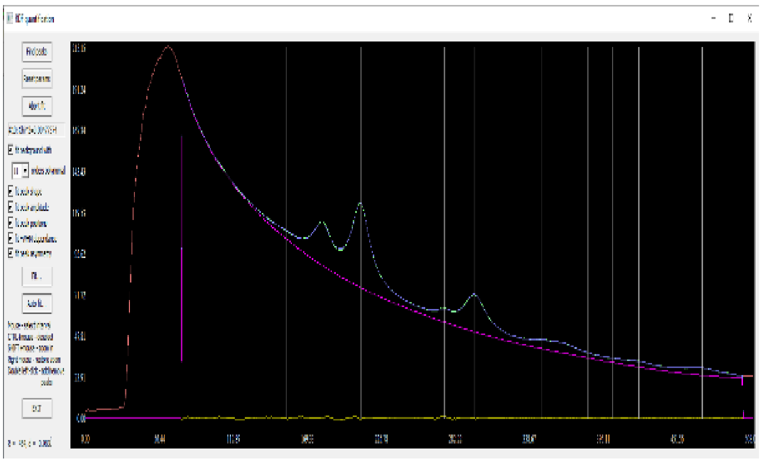

Fig. 5. Extracted profile from diffraction pattern (sample M_8)

Extracted profile shows the presence of a polycrystalline film with diffraction peaks values of 0.292nm, 0.247nm, 0.212nm, 0.163nm, 0.150nm, 0.128nm, 0.122nm, 0.116nm, 0.105nm, 0.095nm; these values are characteristic of a TiC cubic structure[15].

Table 2. Diffraction peaks (sample M_8)

Peak	2 θ (°)	d_{hkl}(Å)	hkl	D_{DS}(nm)
1	0.7254	2.9226		5.1215
2	0.8558	2.4774	111	5.0190
3	0.9954	2.1299	200	5.1015
4	1.2996	1.6314		4.7892
5	1.4076	1.5062	220	4.0821
6	1.6507	1.2844	113	3.7105
7	1.7277	1.2272	222	3.3873
8	1.8155	1.1678		3.0672
9	1.9058	1.1125		2.7834
10	2.0013	1.0594	400	2.5240
11	2.2299	0.9508	420	2.7109
			Mean value =	3.8451

Fig. 6 contains the extracted profile from diffraction pattern for sample C_7 (substrat deposition temperature - room temperature).

Electron diffraction shows the presence of a polycrystalline film with diffraction peaks values of 0.242nm, 0.212nm, 0.149nm, 0.123nm; these values are characteristic of a TiC cubic structure[15].

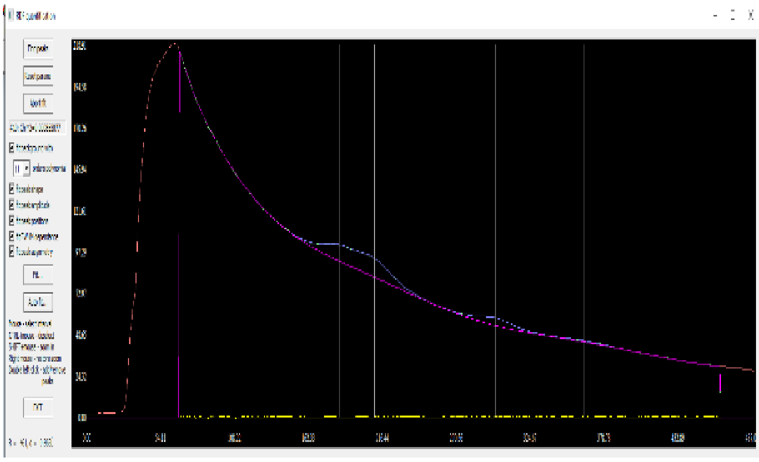

Fig. 6. Extracted profile from diffraction pattern (sample C_7)

The crystal sizes obtained by Scherrer method are given in Table 3.

Table 3. Diffraction peaks (sample C_7).

Peak	2 θ (°)	d_{hkl}(Å)	hkl	D_{DS}(nm)
1	0.8750	2.4229	111	2.9311
2	0.9970	2.1264	200	2.9035
3	1.4177	1.4955	220	2.8737
4	1.7236	1.2301	222	2.7222
			Mean value =	2.8576

3.2. Tribological measurements

Tribological measurements were performed using a ball-on-disc tribometer, with normal force of 0.5N, 1N, 2N and 3N respectively, a stainless steel ball with a dry sliding distance of 30m, and linear speed of 20cm/s. A comparative view of friction coefficient of C-Ti multilayer films at different loading forces for samples M_9 (300C substrat deposition temperature) and M_{11} (300c, Ub=-700V acceleration voltage) respectively is presented in FIGURE 7. For the multilayer samples there is a clear view of the variation of the friction coefficient as the ball reaches deeper into layer and even the transition between C and Ti is visible. This transition indicates an increase of friction coefficient from ~0.3 for the Ti layers to ~0.6 for the C layers. Also, it is visible the fact that applying the acceleration voltage leads to a attenuation of the friction coefficient leap from C to Ti, suggesting that under these condition there is a slight intermixing of the layers.

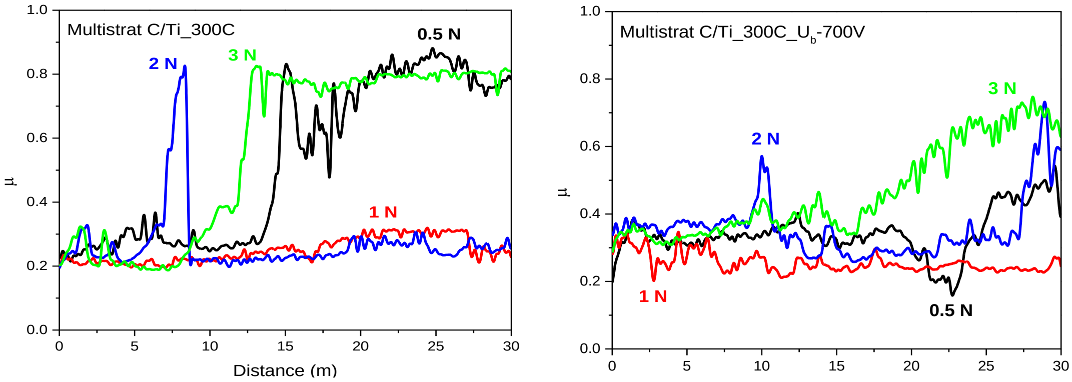

(a) *(b)*

Fig. 7. Comparative view of friction coefficient of C-Ti multilayer films at different loading forces for sample M_9(a) and sample M_{11}(b) respectively.

In the case of composite samples, there is a continuous increase of the coefficient as the sliding ball reaches deeper in the film, suggesting the fact that lower carbon concentration leads to lower friction coefficient (FIGURE 8). Comparing the composite films obtained at different temperatures, result that higher temperature leads to a lower wear rate, improving the coatings wear behavior. Also we can see an improvement of wear in the case of samples DC (FIGURE 9) comparative with samples C(like we can see in the case of sample C_{10} presented in Figure 8).

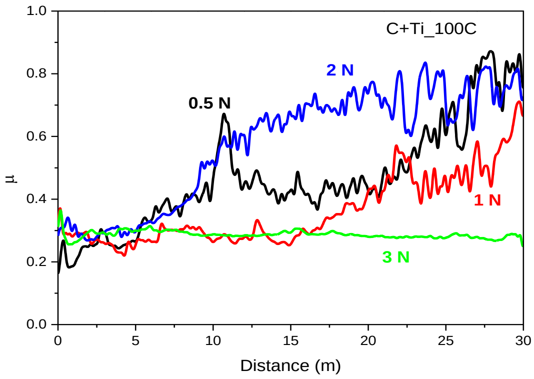

Fig. 8. Friction coefficient of C-Ti composite sample C_{10}(100C substrat deposition temperature) at different loading forces.

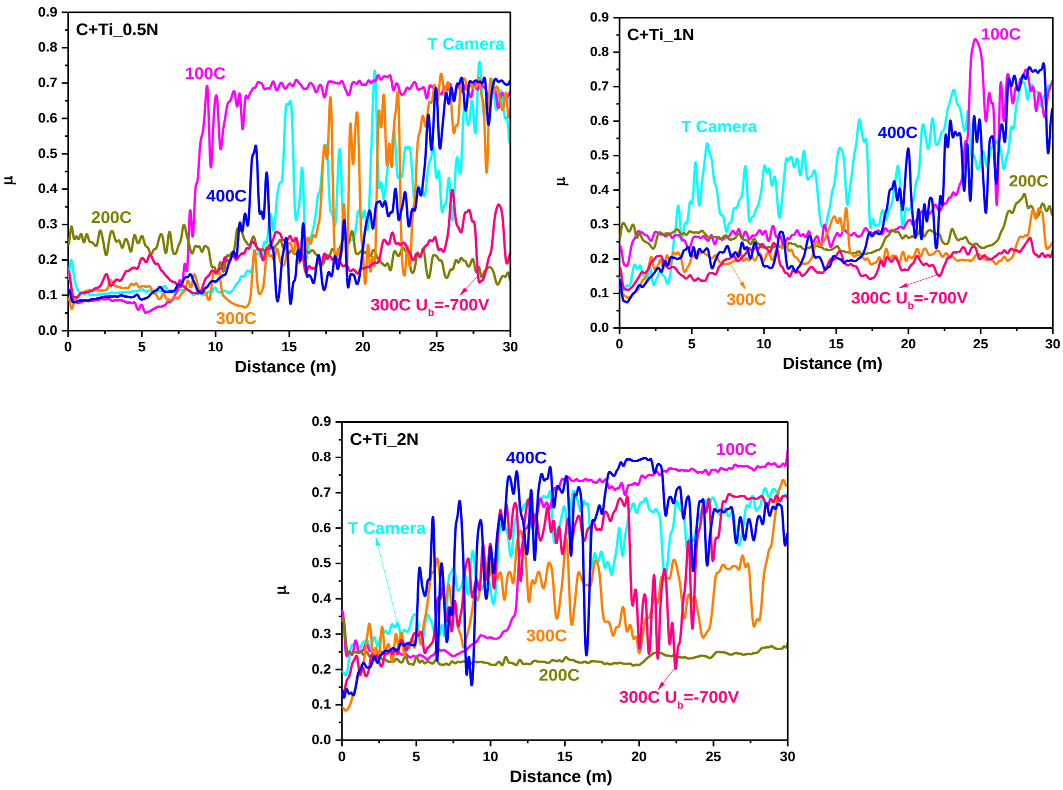

Fig. 9. Friction coefficient vs. distance for samples DC$_1$(room temperature), DC$_2$(100C), DC$_3$,(200C), DC$_4$(300C), DC$_5$(400C), DC$_6$(300C,Ub=-700V), at different loads: 0,5N, 1N, 2N.

3.3. Nanoindentation

The mechanical properties of C / Ti and C-Ti composite films were investigated using a Bruker Hysitron TI 980 TriboIndenter. Were characterised samples DM$_1$(multistrat C-Ti, room temperature deposition temperature), DM$_4$(multistrat C-Ti, 300C deposition temperature) and DC$_1$(composite C/Ti, room temperature deposition temperature).

For each test, several nanoindentations were performed using various types of functions to have a more accurate picture of the hardness and elasticity. The results for Nanoindentation with Partial Unload function (6000µN) is presented in FIGURE 10 in the caseof samples DM$_1$, DM$_4$ and DC$_1$.

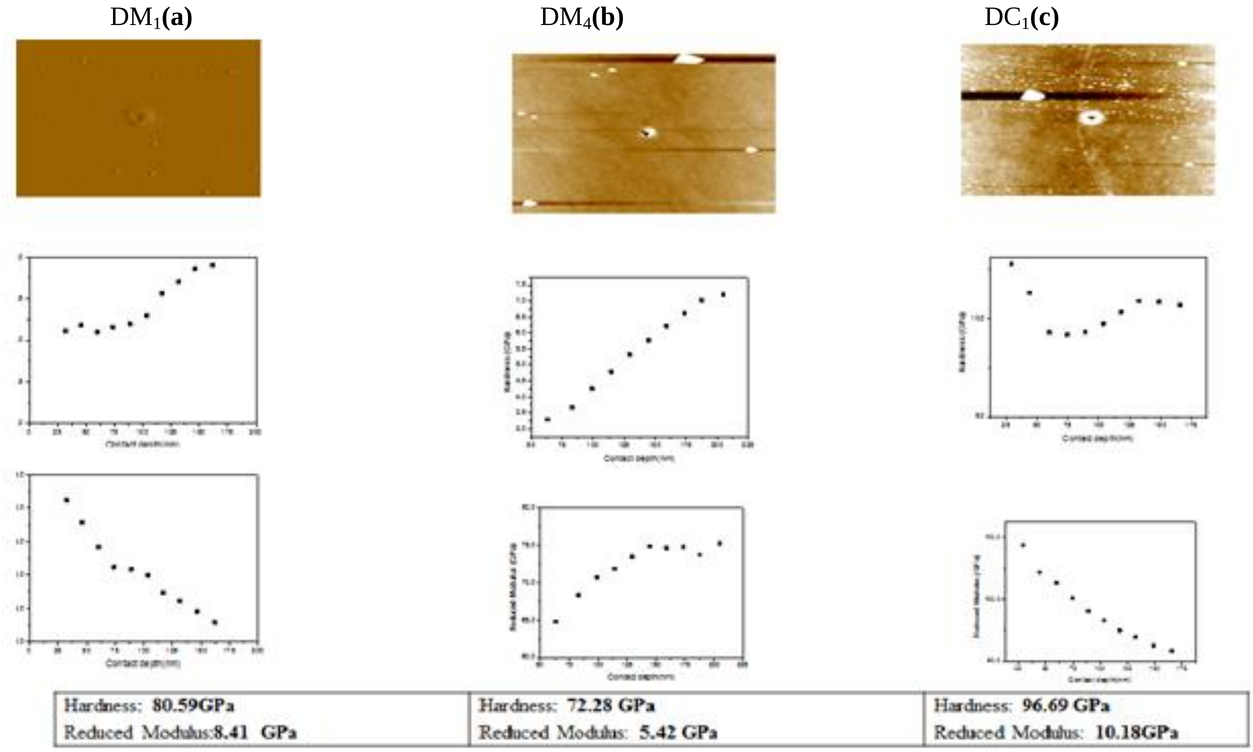

Fig. 10. Hardness and Elastic modulus vs. Conatact depth (sample: DM_1(a), DM_4(b), DC_1(c)).

Figure 10 show that in the case of C-Ti multistrat samples(DM_1 and DM_4), increasing of deposition temperature determine a decreasing of Hardness and Reduced Modulus. On the other hand, we can see that both Hardness and Elastic Modulus are higher in the case of compozit sample DC_1 compared with multistrat samples.

3.4. Electrical measurements

Electrical surface resistance of carbon-titanium multilayer coating on silicon samples was studied on a temperature range above room temperature. The resistance of the sample was obtained by comparing voltage drop on the sample with the voltage drop on a standard resistance in constant current mode. Electrical resistivity is calculated from electrical resistance using sample geometry and then electrical conductivity.

In Table 4. and Table 5. are given the values of the electrical conductivity σ at different temperatures for sample M_{14}(deposition temperature - room temperature, -700V) and for sample N_2, respectively. Using Wiedemann-Franz low, which link the electrical conductivity with thermal conductivity was calculated the thermal conductivity K (Table 4 and Table 5).

Table 4. Electrical conductivity σ and thermal coductivity K for sample M_{14}.

T(K)	340	350	360	370	380
$\sigma\ (\Omega^{-1}\cdot m^{-1})\cdot 10^3$	2.110	1.521	1.431	1.381	1.102
$K(W\cdot m^{-1}\cdot K^{-1})10^{-2}$	1.750	1.300	1.257	1.246	1.022

Table 5. Electrical conductivity σ and thermal coductivity K for sample N_2

T(K)	300	310	320	330	335
$\sigma\ (\Omega^{-1}\cdot m^{-1})\cdot 10^{3}$	8.613	8.751	8.881	8.901	8.991
$K(W\cdot m^{-1}\cdot K^{-1})10^{-2}$	6.305	6.618	6.935	7.168	7.349

The dependence of electrical conductivity by temperature reveals the metallic character of smple N_2 and the semiconductor character of sample M_{14}.

4. Conclusions

Carbon-Titanium (C-Ti) multilayer composite films were deposited on silicon substrates by means of Thermionic Vacuum Arc (TVA) method. The coated layers consiste of a base layer of Carbon and seven Carbon and Titanium layers deposited alternatively, at different substrate temperature values and different substrate bias voltages values. In another deposition way the films were obtained by codeposition, the composite films having a variable C:Ti atomic ration 9:1 at the interface to 1:9 at the surface.

The GIXRD measurements show in the case of sample M_6(400°C substrat deposition temperature) face-centered cubic phases can be found. If the deposition parameters will be improved, and oxygen will be removed, only Ti-C face-centered cubic phases will be obtained, meaning that all titanium atoms will react with carbon atoms. In the sample C_6(deposited at 400°C) a single polycrystalline phase is found (TiC0.4O0.6, face-centered cubic lattice, space group Fm-3m (225), PDF 04-021-7421). The most promising route to obtain c-TiC as a single phase, seems to be the co-deposition at 400 °C, if oxygen will be removed.

TEM measurements reveal the fact that, the increase of the deposition temperature has as effect an increase of size of the crystallized areas.

From tribological measurements result, for the multilayer samples, a variation of the friction coefficient as the ball reaches deeper into layer and even the transition between C and Ti is visible. This transition indicates an increase of friction coefficient from ~0.3 for the Ti layers to ~0.6 for the C layers. In the case of composite samples, there is a continuous increase of the friction coefficient as the sliding ball reaches deeper in the film, suggesting the fact that lower carbon concentration leads to lower friction coefficient.

Nanoidentation measurements show that increasing of deposition temperature detemine, in the case of mulristrat samples, a decreasing of both Hardness and Elastic Modulus. On the other hand, thees parameters are higher for composite samples compared with multistrat samples.

Electrical surface resistance was measured at different temperatures comparing the voltage drop on the sample studied with the voltage drop on a standard series resistance. The electrical conductivity decreases with the increase of the temperature in the case of sample M_{12} and increase with increase of the temperature in the case of sample N_2. Based on Wiedemann-Franz law the thermal conductivity was calculated using electrical conductivity. Also the temperature coefficient of the resistance was calculated; this coefficient is positive for sample M_{12} and negative in the case of sample N_2.

References

[1] N. Oláh, I. Cora, Z. Horváth, T. Csanádi, A. Sulyok, K. Balazsi, J. Eur. Cer. Soc. 38(7), 2886 (2018); https://doi.org/10.1016/j.jeurceramsoc.2018.02.033

[2] A. P. Rubshtein, A. B. Vladimirov, Y. V. Korkh, Y. Ponosov, S. A. Plotnikov, Surf. Coat. Tech. 309(1), 680 (2016); https://doi.org/10.1016/j.surfcoat.2016.11.020

[3] O. E. Kaipoldayev, G. A. Baigarinova, R. R. Nemkayeva, N. R. Guseinov, Y. S. Mukhametkarimov, K. Tauasarov, O. Y. Prikhodko, J.Nano-lectron.Phys. 11(4), 040031 (2019);

https://doi.org/10.21272/jnep.11(4).04003
[4] Z. C. Hong, H. C. Hsueh, C. Z. Wu, S. T. Shiue, Thin Solid Films 660(1), 899 (2018); https://doi.org/10.1016/j.tsf.2018.02.034
[5] X. Liu, L. Liu, B. Sun, B. Li, X. Ke, J. Meas. Eng. 4(3) 167 (2016); https://doi.org/10.21595/jme.2016.17563
[6] W. Q. Bai, L. Li, X. Wang, F. F. He, D. Liu, G. Jin, J. P. Tu, Surface and Coatings Technology 266(1), 70 (2015); https://doi.org/10.1016/j.surfcoat.2015.02.024
[7] S. Zhang, M. Yan, Y. Yang, Y. Zhang, F. Yan, H. Li, Carbon 151(1), 136 (2019); https://doi.org/10.1016/j.carbon.2019.05.031
[8] E. Torskaya, A. Mezrin, J. C. Sánchez-López, Proc. of the 4th Int. Conf. on Industrial Engineering ICIE 2018, 1003 (2019); https://doi.org/10.1007/978-3-319-95630-5_105
[9] E. Torskaya, A. Mezrin, J. C. Sánchez-López, Proc. of the 4th Int. Conf. on Industrial Engineering ICIE 2018, 1011 (2019); https://doi.org/10.1007/978-3-319-95630-5_106
[10] C. P. Lungu, I. Mustata, G. Musa, A. M. Lungu, V. Zaroschi, K. Iwasaki, R. Tanaka, Y. Matsumura, I. Iwanaga, H. Tanaka, T. Oi, K. Fujita, Surface and Coatings Technology 200(1-4), 399 (2005); https://doi.org/10.1016/j.surfcoat.2005.02.172
[11] C. P. Lungu, I. Mustata, V. Zaroschi, A. M. Lungu, A. Anghel, P. Chiru, M. Rubel, P. Coad, G. F. Matthews, JET-EFDA contributors, Phys. Scr. T128, 157 (2007); https://doi.org/10.1088/0031-8949/2007/T128/030
[12] C. P. Lungu, I. Mustata, G. Musa, A. M. Lungu, O. Brinza, C. Moldovan, C. Rotaru, R. Iosub, F. Sava, J. Optoelectron. Adv. M. 8(1), 74 (2006).
[13] V. Ciupina, R. Vladoiu, C. Lungu, V. Dinca, M. Contulov, A. Mandes, P. Popov, G Prodan, Eur. Phys. J. D 66(1), 991 (2012); https://doi.org/10.1140/epjd/e2012-20470-5
[14] G. K. Williamson, W. H. Hall, Acta. Metal. 1(1), 22 (1953); https://doi.org/10.1016/0001-6160(53)90006-6
[15] MINCRYST (khamrabaevite-7200).